

The LHC mass limits for the $SU(2)_{L+R}$ vector resonance triplet of a strong extension of the Standard model

Mikuláš Gintner^{*1,2} and Josef Jurán^{†2,3}

¹*Physics Department, University of Žilina, Univerzitná 1, 010 26 Žilina, Slovakia*

²*Institute of Experimental and Applied Physics, Czech Technical University in Prague, Horská 3a/22, 128 00 Prague, Czech Republic*

³*Institute of Physics, Silesian University in Opava, Bezručovo nám. 13, 746 01 Opava, Czech Republic*

Abstract

In this paper, we derive the mass exclusion limits for the hypothetical vector resonances of a strongly interacting extension of the Standard model using the most recent upper bounds on the cross sections for various resonance production processes. The $SU(2)_{L+R}$ triplet of the vector resonances under consideration is embedded into the effective Lagrangian based on the non-linear sigma model with the 125-GeV $SU(2)_{L+R}$ scalar singlet. No direct interactions of the vector resonance to the SM fermions are assumed. We find that among eleven processes considered in this paper only those where the vector resonances decay to WW and WZ provide the mass exclusion limit. Depending on the values of other parameters of the model the mass limit can be as low as 1 TeV.

1 Introduction

Even though the LHC experiments ATLAS and CMS achieved a spectacular success by discovering the 125 GeV Higgs boson [1] it was more the beginning rather than the end of the struggle to uncover the character of physics beyond the Standard Model (SM). To this moment, it has not been settled down whether new physics takes the form of weakly coupled supersymmetry or strongly coupled composites; in a sense, this problem can be squeezed into the question whether the observed Higgs boson is a fundamental field or a bound state of hypothetical new strong interactions.

If the Higgs is generated as a composite state by new strong interactions the extension of the SM can be effectively described by higher dimensional operators that do not

^{*}gintner@fyzika.uniza.sk

[†]josef.juran@cern.ch

decouple in the low-energy limit. Presumably, they would modify the SM couplings of the Higgs boson with the heavy SM fields, such as the electroweak (EW) gauge bosons and/or the third quark generation. However, while the light SM Higgs boson can guarantee unitarity of the SM to virtually arbitrary high energies, this is not true anymore if the Higgs couplings become anomalous [2, 3]. Nevertheless, the least one could require from the successful effective description of the composite state phenomenology is that it will not break down at energy below the compositeness scale. Meeting this expectation might be assisted with by the presence of additional new composite states which naturally occur in strongly interacting theories.

Consequently, the search for new vector (and other) resonances has its rightful and important place in the ATLAS and CMS collaboration's activities. While no discovery has been made yet, the direct exclusion limits constantly improve. Unfortunately, the vector resonance limits are strongly model and parameter dependent and the mass exclusion limits found in the literature cover only some of the interesting cases. To the best of our knowledge they do not apply to the case considered in this paper.

In this paper, the predictions for the hypothetical neutral and charged vector resonance production cross sections times branching ratios of their various decay channels are calculated and compared to the most recent upper bounds on this observable obtained by the ATLAS and CMS Collaborations. Whenever the predictions exceed the bounds the exclusion limits for the vector resonance masses are inferred.

The effective description of the vector resonance triplet we work with is a rather simplistic view of what might be observed at the LHC beyond the 125 GeV Higgs boson. In this description, the Higgs boson is a scalar composite state followed in the mass hierarchy by a vector composite $SU(2)$ triplet state. In particular, the Higgs sector of the effective Lagrangian under consideration is based on the non-linear sigma model with the 125-GeV $SU(2)_{L+R}$ scalar singlet complementing the non-linear triplet of the Nambu-Goldstone bosons. The new vector resonances are explicitly present in the form of an $SU(2)_{L+R}$ triplet. This setup fits the situation when the global $SU(2)_L \times SU(2)_R$ symmetry is broken down to $SU(2)_{L+R}$.

The vector triplet is introduced as a gauge field via the hidden local symmetry approach [4]. Consequently, the mass eigenstate representation of the vector resonance contains the admixture of EW gauge bosons. It results in the appearance of the mixing-generated (indirect) couplings of the vector triplet with all SM fermions. The gauge sector of this effective description is equivalent to the gauge sector of highly-deconstructed Higgsless model with only three sites [5].

The effective model admits the introduction of the direct coupling of the vector resonance to the SM fermions. We have suggested and thoroughly investigated the possibility with the direct chiral coupling exclusive to the third quark family in our previous works [6, 7, 8]. The model went under the name of tBESS. For the parameters of this model, we have established the limits based on the low-energy data [6, 7] as well as on the most recent LHC measurements [8]. We use these limits to motivate the choice of numerical values throughout this paper. Nevertheless, in this paper, we will restrict our predictions to the case of no direct interactions. Turning the direct interactions on makes the phenomenology of the model much richer. Its investigation will become subject of our following studies.

Under the given assumptions, we calculate the model's production cross section considering the Drell-Yan as well as the vector boson fusion production processes with eleven decay channels of the vector resonances. Namely, these are WW , ZW , WH , ZH , jj , $\ell\ell$, $\ell\nu$, $\tau\tau$, bb , tt , and tb channels. The cross sections are calculated as the functions of the vector resonance mass M_ρ in the region allowed by the validity of the utilized approximations and for various values of g'' spanning the interval allowed by the limits found in [8].

The preliminary evaluations of these cross sections for several selected values of g'' and M_ρ and for all listed decay channels but the $\tau\tau$ and bb ones appeared as a part of our recent publication [8]. There, the comparison of the cross sections to the experimental bounds based on the ATLAS and CMS analyses of up to about 13 fb^{-1} of 13 TeV data published mostly in the middle of 2016 were performed and the mass exclusion limits derived wherever possible. Here, we upgrade this analysis in several aspects. First of all, some improvements on the calculations of the cross sections in [8] have been introduced. They concern mainly the choice of more appropriate parton distribution and vector boson fusion luminosity functions. The improvements were a necessary step before undertaking any more complex analysis. Nevertheless, as we report in [9] they have not resulted in any unexpected discrepancies with the preliminary estimates found in [8].

Secondly, where available the predicted cross sections are compared to the full 2016 data bounds based on about 36 fb^{-1} of integrated luminosity. The comparison results in the most up to date exclusion mass limits for the vector resonances under considerations. In addition, the $\tau\tau$ and bb channel experimental bounds – not available before – are also considered in this paper.

In next Section we will briefly overview the phenomenology of our effective model. In Section 3 the procedure for the calculation of the production cross section will be recapitulated. Section 4 will show the results obtained for various final state. The predictions will be compared with the most recent experimental boundaries. Finally, Section 5 will present the conclusions of our paper.

2 The effective Lagrangian and its phenomenology

The effective Lagrangian, we use in this paper, is the model we studied thoroughly in [6, 7, 8]. It serves as the effective description of the LHC phenomenology of a hypothetical strongly interacting extension of the SM where the principal manifestation of this scenario would be the existence of a vector resonance triplet as a bound state of a new strong interactions. The Lagrangian is built to respect the global $SU(2)_L \times SU(2)_R \times U(1)_{B-L} \times SU(2)_{HLS}$ symmetry of which the $SU(2)_L \times U(1)_Y \times SU(2)_{HLS}$ subgroup is also a local symmetry. The $SU(2)_{HLS}$ symmetry is an auxiliary gauge symmetry invoked to accommodate the $SU(2)_{L+R}$ triplet of new vector resonances. Each of the gauge groups is accompanied by its gauge coupling: g, g', g'' , respectively. Beside the scalar singlet representing the 125 GeV Higgs boson and the hypothetical vector triplet, the effective Lagrangian is built out of the SM fields only.

In the flavor eigenstate basis, the deviations from the SM interactions of the gauge bosons and the vector resonance with the Higgs boson are parametrized by combinations

of two parameters, a_V and a_ρ . In the mass basis, the EW gauge boson to Higgs vertices depend predominantly on a_V . To a high precision, the analogical couplings of the vector resonance triplet to the Higgs boson are parametrized solely by a_ρ . The interaction Lagrangian terms for this sector along with the calculations of the LHC experimental limits for a_V and a_ρ can be found in [8].

The way the description of the vector resonance is introduced implies the mixing between the resonance and electroweak gauge boson fields. The mixing induces the (indirect) couplings between the vector resonance and fermions that are proportional to $1/g''$. Even though the considered symmetry also admits the introduction of the direct interactions of the vector resonance with fermions we will restrict our analysis to the situation when the vector resonance couples to fermions only via the mixing induced interactions.

The masses of the charged and neutral vector resonances in the model are virtually degenerate. The leading order formula for the mass reads

$$M_\rho = \frac{\sqrt{\alpha}g''}{2}v, \quad (1)$$

where α is a dimensionless free parameter emerging in the effective Lagrangian and v is the electroweak symmetry breaking scale. Usually, α is traded off for M_ρ so that the latter can serve as one of the free parameters of the model. Our previous studies of the low-energy limits [6, 7] as well as the Higgs-related limits and the unitarity limits [8] suggest that we should consider $M_\rho \geq 1$ TeV and $10 \leq g'' \leq 20$.

The Higgs-related parameters a_V and a_ρ influence significantly only decay channels of very small branching ratios. Hence, their impact on the cross sections calculated in this paper is very negligible. Thus, throughout this paper, we will use $a_V = 1$ (the SM case) and $a_\rho = 0$ (no Higgs-to-vector resonance coupling). These values are quite close to one of the experimentally preferred points of the parameter space [8].

In the case of no direct interactions of the vector resonance with fermions, the total decay width of the resonance can be well approximated by

$$\Gamma_\rho = \frac{1}{48\pi v^4} \frac{M_\rho^5}{g''^2}. \quad (2)$$

In Fig. 1 we depict how the vector resonance total width depends on the resonance mass and g'' . At the same time, the graph shows the width-to-mass ratio contours. This information will be important later in the paper when the region of the validity of the used approximations is considered.

3 The production cross section calculations

We are interested in the LHC cross sections of the two-particle final state processes that would proceed via the vector resonance production. We calculate the cross section $\sigma(pp \rightarrow ab + X)$ using the Narrow Width Approximation (NWA), i.e. as the product of the on-shell production cross section of the resonance, σ_{prod} , and the branching ratio for the vector resonance decay channel under consideration

$$\sigma(pp \rightarrow ab + X) \stackrel{\text{NWA}}{=} \sigma_{\text{prod}}(pp \rightarrow \rho + X) \times \text{BR}(\rho \rightarrow ab). \quad (3)$$

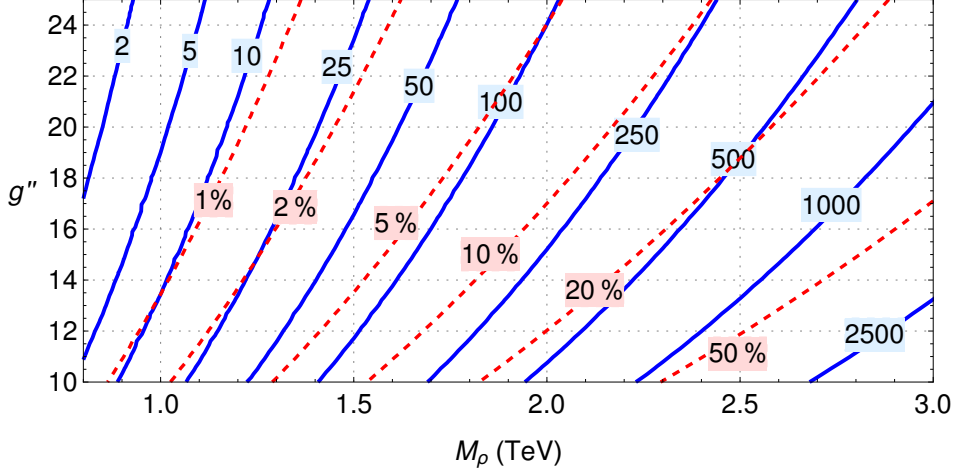


Figure 1: The solid lines represent the contours of the total decay width of the vector resonance (labeled in GeV) in the $g'' - M_\rho$ parameter space. The dashed lines represent the width-to-mass ratio of the vector resonance (labeled in percents). No direct interactions of the resonance to fermions are assumed.

As the name suggests the NWA works when $\Gamma_\rho \ll M_\rho$. It also ignores the signal-background interference effects. The influence of these effects on the precision of the approximation have been inspected in [10].

The production cross section of a resonance can be expressed as

$$\sigma_{\text{prod}}(pp \rightarrow \rho + X) = \sum_{i \leq j \in p} 16\pi^2 K_{ij} \frac{\Gamma_{\rho \rightarrow ij}}{M_\rho} \frac{dL_{ij}}{d\hat{s}} \Big|_{\hat{s}=M_\rho^2}, \quad (4)$$

where i, j run through all partons of the colliding protons and $\Gamma_{\rho \rightarrow ij}$ is the partial decay width of the resonance to the partons i and j . Furthermore, $dL_{ij}/d\hat{s}$ is the luminosity of the colliding partons, and

$$K_{ij} = \frac{2J+1}{(2S_i+1)(2S_j+1)} \frac{C}{C_i C_j}, \quad (5)$$

where J is the spin of the resonance, C is its color factor, and S_i, S_j and C_i, C_j are the spins and colors of the initial partons, respectively. Note that a model dependence enters the production cross section (4) virtually¹ only via the partial decay width $\Gamma_{\rho \rightarrow ij}$.

Two dominant production mechanisms for the triplet of our vector resonances are the Drell-Yan (DY) and the vector boson fusion (VBF) processes. We will consider them both in our analysis. For the sake of simplicity, in our calculations of the production cross sections the proton contents is reduced down to the up and down quarks².

¹ In principle, the parton-parton luminosity is also sensitive to new physics via modifications of the SM couplings and the parton distribution functions. Nevertheless, we expect these effects to be negligible and ignore them in our analysis.

² We do not expect that this approximation would significantly influence conclusions when there are no direct interactions of the vector resonance to fermions.

In the DY case, the parton-parton luminosity in (4) is defined as

$$\frac{dL_{ij}}{d\hat{s}} = \frac{1}{s} \int_{\tau}^1 \frac{dx}{x} \frac{1}{1 + \delta_{ij}} [f_i(x, \hat{s}) f_j(\tau/x, \hat{s}) + i \leftrightarrow j], \quad (6)$$

where s and \hat{s} are the squared center of mass energies of the colliding protons and partons, respectively, $\tau = \hat{s}/s$, and f_i is a parton distribution function of the i th parton with the momentum fraction x of its proton's momentum.

The VBF production will be calculated in the Effective W Approximation (EWA) [11]. When the EWA is applied to the VBF case, the W and Z bosons are also treated as partons in the proton. The VBF luminosity can be expressed as

$$\begin{aligned} \frac{dL_{V_m V_n [pp]}}{d\tau} &= \sum_{i \leq j} \frac{1}{1 + \delta_{ij}} \int_{\tau}^1 \frac{dx_1}{x_1} \int_{\tau/x_1}^1 \frac{dx_2}{x_2} \\ &\times [f_i(x_1, q^2) f_j(x_2, q^2) \frac{dL_{V_m V_n [q_i q_j]}}{d\hat{\tau}} + i \leftrightarrow j], \end{aligned} \quad (7)$$

where $\hat{\tau} = \tau/(x_1 x_2)$, and $dL_{V_m V_n [q_i q_j]}/d\hat{\tau}$ is the luminosity for two vector bosons V_m and V_n emitted from i th and j th quarks, respectively. In the EWA, the latter can be obtained analytically assuming that the gauge bosons are emitted on-shell and in small angles to their parental quarks. Also, if the gauge bosons fuse to a heavy resonance their masses should be negligibly small compare to the resonance mass. In this approximation, the transversal and longitudinal polarizations of the emitted gauge bosons are considered as separate modes. Since the longitudinal mode usually dominates in the presence of the deviations from the SM, we use the longitudinal mode only in our calculations.

The luminosity for two longitudinal vector bosons V_m and V_n emitted from i th and j th quarks reads

$$\frac{dL_{V_m^L V_n^L [q_i q_j]}}{d\hat{\tau}} = \frac{v_{m[i]}^2 + a_{m[i]}^2}{4\pi^2} \frac{v_{n[j]}^2 + a_{n[j]}^2}{4\pi^2} \frac{1}{\hat{\tau}} [(1 + \hat{\tau}) \log(1/\hat{\tau}) - 2(1 - \hat{\tau})], \quad (8)$$

where $v_{m[i]}$ and $a_{m[i]}$ are the vector and axial couplings of the gauge boson V_m to the quark current q_i . In particular,

$$v_{W[q_i]} = -a_{W[q_i]} = \frac{g}{2\sqrt{2}} \quad (9)$$

for any q_i , and

$$v_{Z[u]} = \frac{g}{4c_W} (1 - \frac{8}{3}s_W^2), \quad a_{Z[u]} = \frac{g}{4c_W}, \quad (10)$$

$$v_{Z[d]} = -\frac{g}{4c_W} (1 - \frac{4}{3}s_W^2), \quad a_{Z[d]} = -\frac{g}{4c_W}, \quad (11)$$

where $s_W = \sin \theta_W$ and $c_W = \cos \theta_W$.

For the numerical evaluation of the parton-parton luminosity we used the Mathematica [12] package Mane Parse [13] with the PDF set CT10 from the LHAPDF 6 library at HepForge repository [14]. The obtained parton-parton luminosities for both production mechanisms of the new vector resonance at the LHC ($\sqrt{s} = 13$ TeV) are depicted in Fig. 2.

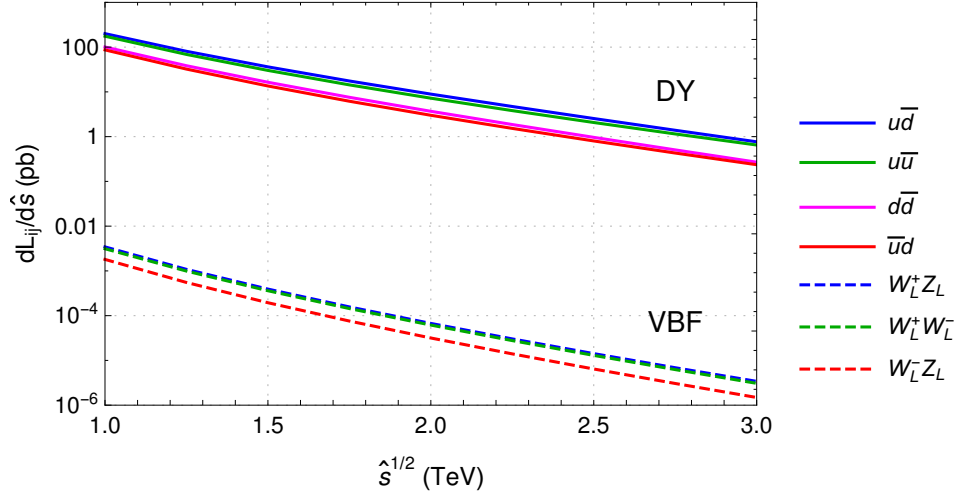


Figure 2: The parton-parton luminosities for the DY (solid lines) and longitudinal VBF (dashed lines) production in the proton-proton collisions at $\sqrt{s} = 13$ TeV. The CT10 set of parton distribution functions was used.

4 The vector resonance mass limits and the upper bounds on $\sigma(pp \rightarrow \rho + X) \times \text{BR}$

Once the production cross sections have been evaluated, we are a single step from finalizing the predictions of the LHC cross sections of the processes under investigation. The final step involves the multiplication of the production cross section by an appropriate branching ratio (see Eq. (3)). When the direct interactions of the vector resonances are considered, the BR endows the resulting cross section with the sensitivity to the corresponding model's parameters.

We can evaluate how the existing ATLAS and CMS data restrict our model when we compare its predictions to the upper bounds on the resonance production cross section times the branching ratios for various decay channels. The bounds are rather model independent once spin of the resonance under consideration is specified. Of course, one should keep in mind that the calculations involved proceed under the assumption of a narrow-width resonance. As can be seen in Fig. 1, increasing M_ρ takes us away from the NWA region. Consequently, our cross section predictions become less reliable. On the other hand, as M_ρ grows the cross sections also depart from the experimental bounds. Thus our predictions of the cross sections can serve their purpose even at a higher mass to a certain extent. Nevertheless, we do not consider as meaningful to go beyond $M_\rho = 3$ TeV in our analysis.

As we will see below the WW and WZ channels are the only ones among those investigated in this paper in which the current data restrict our model. The restrictions can be translated into the lower exclusion bounds on the vector resonance mass.

4.1 The WW and WZ channels

In the absence of the direct couplings of the vector resonance triplet to fermions the decay widths of the neutral and charged vector resonances are dominated by their decays to the EW gauge bosons: $\text{BR}(\rho \rightarrow WW/WZ) > 99\%$.

In Fig. 3, we present the cross section times branching ratios for the WW and WZ decay channels of our model at the LHC collision energy of 13 TeV. The predictions are given for three different values of g'' , namely 10, 15, and 20. The g'' values were chosen to span the region allowed by the combination of the limits obtained in [8]. In addition, the most restrictive upper 95% C.L. experimental bounds on the cross section times branching ratio are superimposed in the graphs. In fact, since the current experimental data do not contradict the expectation curves we take the latter as the established experimental boundary.

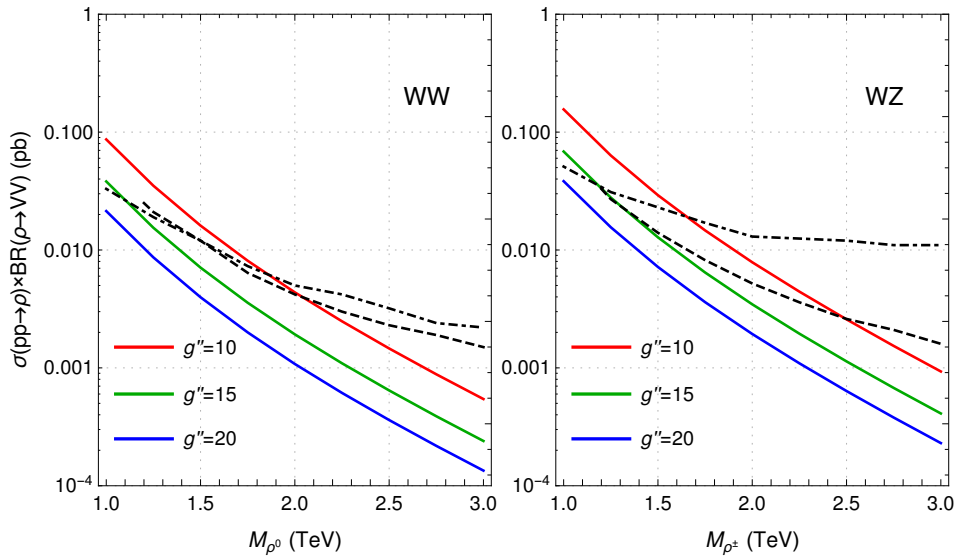


Figure 3: The 13 TeV cross section times branching ratios of our model for the WW (left panel) and WZ (right panel) decay channels at $g'' = 10$ (solid upper red), 15 (solid middle green), and 20 (solid bottom blue). In both panels, the experimental 95% C.L. upper limit dashed curves are based on the dijet final state data (35.9 fb^{-1}) [15]. The dot-dashed WW and WZ curves are based on the semileptonic final state data (13.2 fb^{-1}), [16] and [17], respectively.

In the WW channel, the experimental upper bounds [15, 16] exclude the mass of the neutral vector resonance below about 2.1 TeV and 1.1 TeV for $g'' = 10$ and 15, respectively. The $g'' = 20$ case is not restricted above 1 TeV. In the WZ , the experimental upper bounds [15, 17] exclude the mass of the charged vector resonance below about 2.5 TeV and 1.3 TeV for $g'' = 10$ and 15, respectively. Again, the $g'' = 20$ case is not restricted above 1 TeV. In our model, the neutral and charged vector resonances are virtually degenerate in their masses. Therefore, within the model, the stronger exclusion mass limit on the charged resonance can be considered as the limit for the neutral resonance, as well.

While we do not consider the direct interactions of the vector resonance with fermions in this paper, we can briefly estimate the effect of the direct interaction with the third

quark generation as it was introduced in our tBESS model [6, 7]. There, the corresponding chiral couplings were parameterized by the $b_{L,R}$ free parameters. Setting $b_{L,R}$ to their maximally low-energy precision data allowed values — $b_{L,R} \approx 0.1$ [7] — can lower $\text{BR}(WW)$ of the 1 TeV resonance down to about 70% for $g'' = 10$, to 30% for $g'' = 15$, and to 12% for $g'' = 20$. In the 2 TeV resonance case, $\text{BR}(\rho \rightarrow WW)$ would be lowered to about 97%, 87%, and 67%, respectively. Thus, the direct fermionic interactions of the vector resonance can noticeably decrease the cross section predictions (and, thus, release the experimental restrictions) of the model in this channel. The similar effect occurs in the ZW channel. When $M_\rho = 1$ TeV and $b_{L,R} = 0.1$, $\text{BR}(WZ)$ gets lowered to about 71%, 31%, and 12% for $g'' = 10, 15$, and 20, respectively. For $M_\rho = 2$ TeV, the corresponding BR's read 97%, 87%, and 67%.

4.2 The bb , tt , and tb channels

In the left panel of Fig. 4, we present the cross section times branching ratio for the bb channel of our model at the LHC collision energy of 13 TeV. In the middle panel, there is the prediction for the tt channel shown. The tb channel is depicted in the right panel of Fig. 4. There, the sum of the $t\bar{b}$ and $b\bar{t}$ contributions is considered. The predictions

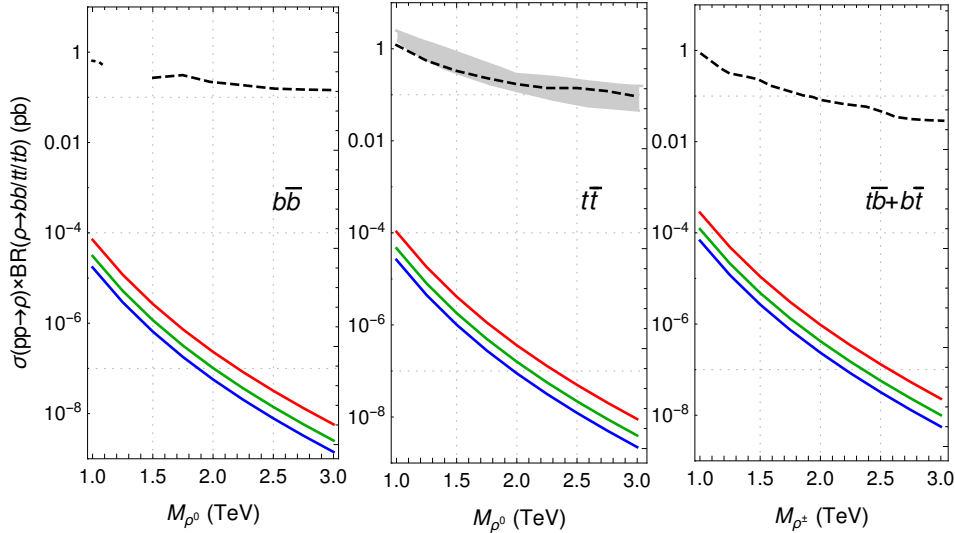


Figure 4: The 13 TeV cross section times branching ratios of our model for the bb (left panel), tt (middle panel), and tb (right panel) decay channels at $g'' = 10$ (solid upper red), 15 (solid middle green), and 20 (solid bottom blue). In the bb channel, the experimental 95% C.L. upper limit curves are based on 3.2 fb^{-1} [18] (dotted) and 13.3 fb^{-1} [19] (dashed) of data. In the tt channel, the bounds are based on the 2.6 fb^{-1} lepton+jets & fully hadronic final states [20] (gray stripe) and the 3.2 fb^{-1} lepton+jets final state [21] (dashed). Finally, the tb channel experimental limit originate from the 35.9 fb^{-1} lepton+jets final state [22] (dashed).

are given for $g'' = 10, 15$, and 20. When there is no direct interaction the predicted cross sections in these channels are not far from each other. In the bb and tt channels, the existing upper experimental bounds [18, 19, 20, 21] are several orders of magnitude

above the predicted cross sections. The same situation can be found in the tb channel (for the experimental upper bounds for this channel, see [22]). Thus there are currently no exclusion limits on the no-direct-interaction version of our model resulting from these channels.

However, once the direct interaction to the third quark family is turned on the bb , tt and tb channels will be affected the most. For example, setting $b_{L,R} = 0.1$ the branching ratios for these channels increase from $\text{BR}(bb) = 0.08\%(0.005\%)$, $\text{BR}(tt) = 0.12\%(0.008\%)$, and $\text{BR}(tb) = 0.18\%(0.012\%)$ for $M_\rho = 1$ TeV (2 TeV), to the values ranging in $15\%(1.4\%) \leq \text{BR}(bb) \leq 44\%(17\%)$, $14\%(1.3\%) \leq \text{BR}(tt) \leq 44\%(16\%)$, and $29\%(2.7\%) \leq \text{BR}(tb) \leq 87\%(33\%)$ when $10 \leq g'' \leq 20$. Yet it does not seem to be enough to obtain any exclusion limits from the latest measurements.

4.3 The remaining channels

Beside the channels discussed above we have also calculated predictions for the following channels: ZH , WH , jj , $\ell\ell$, $\ell\nu$, and $\tau\tau$, where $\ell = e, \mu$. In all these remaining channels,

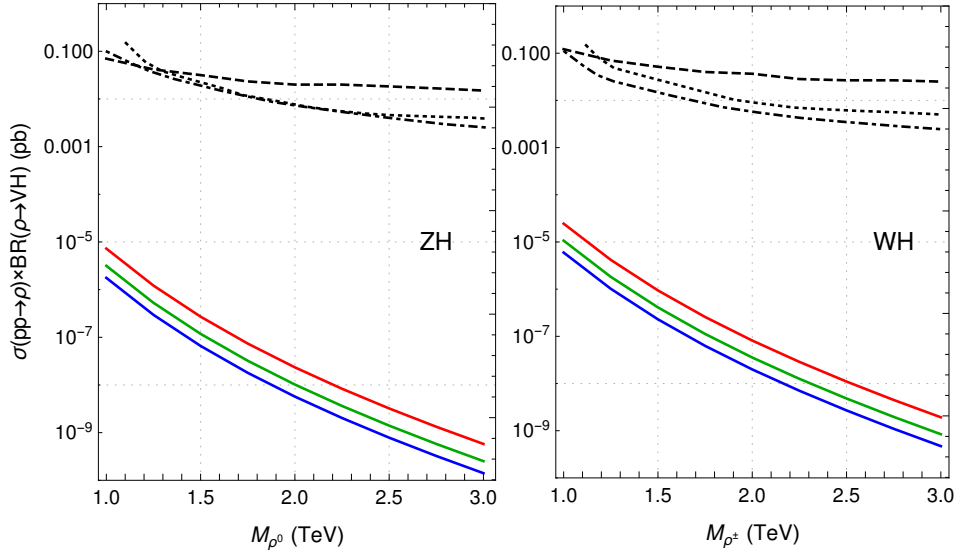


Figure 5: The 13 TeV cross section times branching ratios of our model for the ZH (left panel) and WH (right panel) decay channels at $g'' = 10$ (solid upper red), 15 (solid middle green), and 20 (solid bottom blue). The experimental upper bounds shown in both panels originate from the following measurements: the ATLAS $36.1 \text{ fb}^{-1} qqbb$ final state [23] (dotted), the CMS $35.9 \text{ fb}^{-1} qqbb$ final state [24] (dot-dashed), and the ATLAS $3.2 \text{ fb}^{-1} \ell\ell bb + \nu\nu bb / \ell\nu bb$ final state [25] (dashed).

the predicted cross sections are too low when compared to even most recent experimental upper bounds. This can be seen in Figs. 5, 6, and 7. Thus there are no exclusion limits implied by these channels. The introduction of the third quark family direct coupling will decrease the individual branching ratios of these channels by the same factors as in the case of the WW/WZ channels. Therefore, no mass exclusion limits can emerge with this modification.

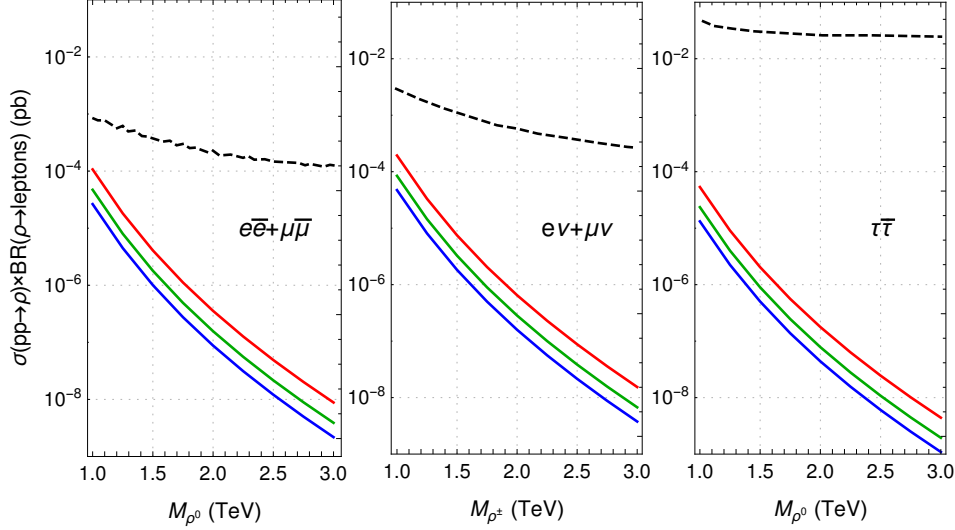


Figure 6: The 13 TeV cross section times branching ratios of our model for $e^+e^- + \mu^+\mu^-$ (left panel), $e^+\nu_e + \mu^+\nu_\mu + \text{c.c.}$ (middle panel) and $\tau^+\tau^-$ (right panel) decay channels at $g'' = 10$ (solid upper red), 15 (solid middle green), and 20 (solid bottom blue). The experimental upper bounds (dashed) for $e^+e^- + \mu^+\mu^-$ are based on 36.1 fb^{-1} of data [26], on 36.1 fb^{-1} of data for $e^+\nu_e + \mu^+\nu_\mu + \text{c.c.}$ [27], and on 2.2 fb^{-1} of data for $\tau^+\tau^-$ [28].

5 Conclusions

We have studied the production cross section times branching ratio for various decay channels in the productions of hypothetical neutral and charged vector resonances of new strong physics origin. The resonances have been introduced in the context of the phenomenological Lagrangian where beside the composite 125 GeV Higgs boson the $SU(2)_{L+R}$ triplet of composite vector resonances is explicitly present. The ESB sector of our effective Lagrangian has been based on the $SU(2)_L \times SU(2)_R \rightarrow SU(2)_{L+R}$ non-linear sigma model while the scalar resonance has been introduced as the $SU(2)_{L+R}$ singlet. The vector resonance has been built in employing the hidden local symmetry approach. While allowed by the symmetry of the Lagrangian no direct fermion interactions of the vector resonance triplet have been considered. The only interactions of the resonance to fermions have been those generated by the mixing with the EW gauge bosons.

We have compared the model's predictions with the upper bounds on the production cross section times branching ratio obtained by the ATLAS and CMS Collaborations from the full 2016 data sets. We have found that the WW (WZ) channel excludes the mass of the neutral (charged) vector resonance below about 2.1 TeV (2.5 TeV) and 1.1 TeV (1.3 TeV) for $g'' = 10$ and 15, respectively. The $g'' = 20$ cases are not restricted above 1 TeV. The direct fermionic interactions of the vector resonance can noticeably decrease the cross section predictions (and, thus, release the experimental restrictions) of the model in these channels.

The predicted cross sections are well below the experimental upper bounds in the bb , tt , and tb channels, as well as in all other channels considered in this paper. The bb , tt , and tb channels would be affected most once the direct fermionic interactions of the vector

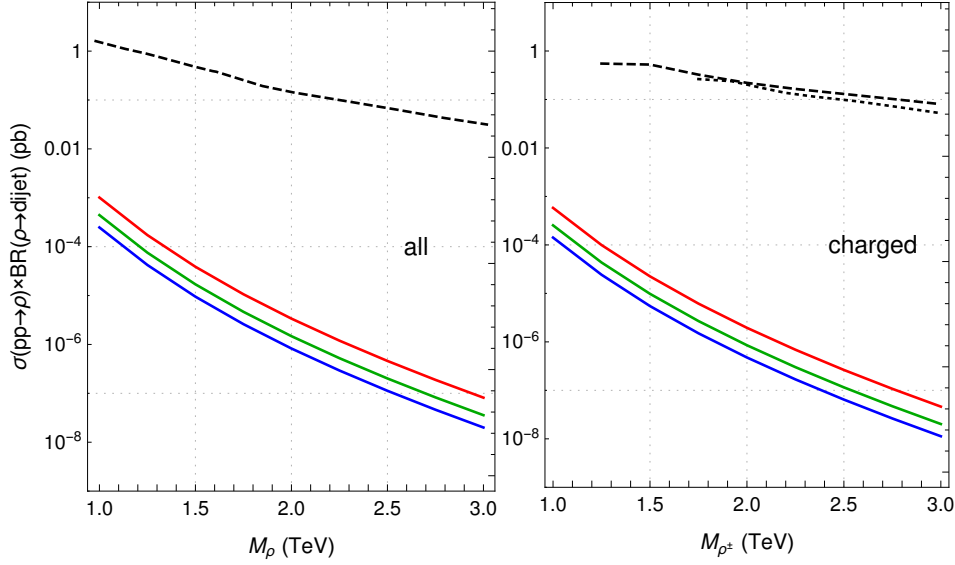


Figure 7: The 13 TeV cross section times branching ratios of our model for the dijet (left panel) and charged dijet (right panel) decay channels at $g'' = 10$ (solid upper red), 15 (solid middle green), and 20 (solid bottom blue). In the left panel, the displayed experimental upper bound below 1.6 TeV is based on 27 fb^{-1} of data and the bound above 1.6 TeV is based on 36 fb^{-1} of data [29] (dashed). In the right panel, the experimental bounds are based on 37 fb^{-1} of data [30] (dotted), and on 15.7 fb^{-1} of data [31] (dashed).

resonance are introduced. Consequently, the predicted cross sections in these channels might increase up to three orders of magnitude. The cross sections in all remaining channels would shrink by the same factor as in the WW and WZ channels.

In summary, the new strong physics vector resonances of the considered type are restricted by the current LHC data significantly weaker than their weakly-interacting counter-parts. The lower exclusion limits will be further relaxed if there are direct interactions of the vector resonances to the third generation quark doublet.

Acknowledgments

We would like to thank Karol Kovařík for useful discussions. The work of M.G. and J.J. was supported by the Grants LTT17018 and LG15052 of the Ministry of Education, Youth and Sports of the Czech Republic. M.G. was supported by the Slovak CERN Fund. J.J. was supported by the National Scholarship Programme of the Slovak Republic.

References

- [1] G. Aad *et al.* (ATLAS Collaboration), Phys. Lett. B **716**, 1 (2012); S. Chatrchyan *et al.* (CMS Collaboration), *ibid.* 30 (2012).

- [2] B. W. Lee, C. Quigg, and H. B. Thacker, Phys. Rev. D **16**, 1519 (1977); Phys. Rev. Lett. **38** (1977) 883.
- [3] M. S. Chanowitz and M. K. Gaillard, Nucl. Phys. **B261**, 379 (1985).
- [4] M. Bando, T. Kugo, and K. Yamawaki, Phys. Rep. **164**, 217 (1988).
- [5] R.S. Chivukula et al, Phys. Rev. D **74**, 075011 (2006).
- [6] M. Gintner, J. Juráň, and I. Melo, Phys. Rev. D **84**, 035013 (2011).
- [7] M. Gintner, J. Juráň, Eur. Phys. J. C **73**, 2577 (2013).
- [8] M. Gintner, J. Juráň, Eur. Phys. J. C **76**, 651 (2016), erratum, Eur.Phys.J. C**77**, 6 (2017).
- [9] M. Gintner, J. Juráň, to be published in Communications – Scientific Letters of the University of Zilina.
- [10] D. Pappadopulo, A. Thamm, R. Torre and A. Wulzer, JHEP 1409 (2014) 060.
- [11] S. Dawson, Nucl.Phys. B 249, 42 (1985).
- [12] Wolfram Research, Inc., Mathematica, Version 10.4, Champaign, IL (2016).
- [13] D.B. Clark, E. Godat, F.I. Olness, arXiv:1605.08012. Mane Parse package download: <https://ncteq.hepforge.org/mma/index.html>
- [14] A. Buckley et al., Eur. Phys. J. C 75, 132 (2015); arXiv:1412.7420. LHAPDF6 PDFs download: <http://lhpdf.hepforge.org/pdfsets>
- [15] CMS Collaboration, CMS PAS B2G-17-001.
- [16] ATLAS Collaboration, ATLAS-CONF-2016-062.
- [17] ATLAS Collaboration, ATLAS-CONF-2016-082.
- [18] ATLAS Collaboration, ATLAS-CONF-2016-031.
- [19] ATLAS Collaboration, ATLAS-CONF-2016-060.
- [20] CMS Collaboration, arXiv:1704.03366.
- [21] ATLAS Collaboration, ATLAS-CONF-2016-014.
- [22] CMS Collaboration, CMS PAS B2G-17-010
- [23] ATLAS Collaboration, ATLAS-CONF-2017-018.
- [24] CMS Collaboration, CMS PAS B2G-17-002.
- [25] ATLAS Collaboration, arXiv:1607.05621.

- [26] ATLAS Collaboration, ATLAS-CONF-2017-027.
- [27] ATLAS Collaboration, ATLAS-CONF-2017-016.
- [28] CMS Collaboration, JHEP 02(2017)048.
- [29] CMS Collaboration, CMS PAS EXO-16-056.
- [30] ATLAS Collaboration, arXiv:1703.09127.
- [31] ATLAS Collaboration, ATLAS-CONF-2016-069.